Model predictive control strategy applied to different types of building for space heating

Gohar Gholamibozanjani[a], Joan Tarragona[b,c], Alvaro de Gracia[b,d], Cèsar Fernández[b], Luisa F. Cabeza[b], Mohammed M. Farid[a*]

[a]Department of Chemical and Materials Engineering, University of Auckland, Private Bag 92019, Auckland, New Zealand

[b]GREiA Innovació Concurrent, INSPIRES Research Centre, University of Lleida, Pere de Cabrera s/n, 25001-Lleida, Spain

[c]CIRIAF – Interuniversity Research Centre on Pollution and Environment Mauro Felli,Via G. Duranti 63, 06125, Perugia, Italy

[d]CIRIAF - Interuniversity Research Centre, University of Perugia, Via G. Duranti 67, 06125 Perugia, Italy

*Corresponding author: m.farid@auckland.ac.nz

ABSTRACT

In recent years, the concept of energy-efficient buildings has attracted widespread attention due to growing energy consumption in different types of buildings. The application of thermal energy storage (TES) systems, especially latent heat energy storage (LHES), has become a promising approach to improve thermal efficiency of buildings and hence reduces CO_2 emissions. One way to achieve this could be by implementing a model predictive control (MPC) strategy, using weather and electricity cost predictions. To this end, a heat exchanger unit containing a phase change material (PCM) as a LHES medium, thermally charged by

solar energy was incorporated into three versions of a standard building. This paper reports on the use of EnergyPlus software to simulate the heating demand profile of these buildings, with Solving Constraint Integer Programs (SCIP) as the optimization tool. After applying the MPC strategy, the energy costs of different building types were evaluated. Furthermore, the effect of the prediction horizon and decision time step of the MPC strategy, and PCM mass capacity on the performance of the MPC were all investigated in 1 and 7-day simulations. The results showed that by increasing the prediction horizon and PCM mass, more cost saving could be obtained. However, in terms of decision time step, although the study revealed that increasing it led to a higher energy saving, it made the system more sensitive to sharp changes as it failed to provide an accurate reading of the parameters and variables.

Keywords: Model predictive control (MPC), active solar heating, latent heat energy storage (LHES), phase change material (PCM), optimization

1. Introduction

About 36% of global energy used worldwide is attributed to buildings [1], which also contribute to about 17% of total direct energy-related CO_2 emissions to the environment [2]. Heating, ventilation, and air conditioning (HVAC) make a major contribution to energy consumption in buildings [3].

Nomenclature

Δp	overall pressure drop (kPa)

Δt	decision time step (s)
ΔT	temperature difference (°C)
C_p	specific heat capacity (kJ/kg·K)
I	intensity of solar radiation (W/m^2)
k	simulation time step
l	cost function (NZD)
M	mass (kg)
$\dot{m}$	mass flow rate
N	number of prediction horizon
Q	volume flow rate (m^3/s)
$\dot{Q}$	thermal power (kJ/s)
T	temperature (°C)
u	control input
U	Constraint of input value
x	control input
x_0	initial state of the control input
X	Constraint of input value

Greek Symbols

η	efficiency
ε	conversion coefficient to estimate the outlet temperature of heat exchanger as a function of PCM temperature

Subscripts

f	fan
amb	ambient
HE-Room	directing from heat exchanger to room
in, SAC	inlet of solar air collector
l	liquid
m	melting point
out, SAC	outlet of solar air collector
out, HE	outlet of heat exchanger
s	solid
SAC-HE	directing from solar air collector to heat exchanger
SAC-Room	directing from solar air collector to room

Design professionals, especially architects and engineers, are experiencing an unprecedented level of demand to apply novel approaches to buildings in order to improve their thermal performance. The integration of thermal energy storage (TES) systems into buildings can satisfy their growing demand for energy, as well as reduce environmental pollution caused by the excessive use of energy. Among different energy storage systems, latent heat energy storage (LHES) using phase change materials (PCMs) can greatly enhance the energy efficiency of buildings owing to their large energy storage capacity, which is available within a narrow temperature range [4]. However, the incorporation of TES in buildings to minimize energy consumption and energy costs, while maintaining a comfortable thermal environment, requires comprehensive pre-analysis and thorough mathematical study.

The development of computer technologies and modeling techniques has enabled the prediction of energy consumption levels in buildings [5]. By means of design control methods using dynamic models, prediction of the thermal performance of building systems is

now more cost-effective and less time-consuming. Indeed, dynamic models have become crucial for the development of control programs to optimize energy consumption and provide a comfort zone for the occupants of buildings [6]. In this regard, smart control of TES would maximize its energy and economic benefits and hence justify its initial high investment costs.

Model predictive control (MPC) through the well-established strategy of classical control has attracted research attention in the area of energy-efficient buildings. Although MPC strategies have been used in process control for several decades, they have not been applied to building automation until recently. Basic criteria that MPC strategies need to meet are simplicity, well-estimated system dynamics, steady-state properties, and suitable prediction properties [7]. For instance, Ebrahimpour and Santro [8] used the moving horizon estimation of lumped load and occupancy in order to improve the accuracy of the dynamic model and MPC performance, subsequently. The advantage of MPC strategy over conventional building control methods is that it considers the future prediction of ambient temperature, solar radiation and occupancy, as well as system operating constraints, in the design of the control system [9]. However, in conventional methods, the control system is based on occupancy status of the building only, so the heating system is switched off if there is no one in the building. Further, TES is not used to cut down the operating cost of the building [10].

By taking into account internal gains, equipment, weather, and cost, an MPC can provide the required level of thermal comfort [11]. Ma et al. [12] conducted a numerical study to control the cooling system of a building. The building was equipped with a water tank and a series of chillers to provide the cold water. A cost saving of about 24% was achieved through implementation of an MPC strategy and using weather profile prediction. Morosan et al. [13] also studied thermal regulation using an MPC strategy and weather profile prediction. The control design in their study was based on available control strategies, which have centralized and decentralized structures. In the centralized structure, a single controller is used to provide

a comfortable indoor temperature for a multi-zone building. However, in the decentralized structure, each zone has its own controller. As the centralized structure has computational complexity, and the decentralized one ignores heat transfer between zones, they proposed a distributed control strategy to take advantage of both control structures. Their findings showed that by implementing the distributed structure, in which case the local controllers of different zones share their future behavior, the performance of system was improved.

MPC strategy is being used in HVAC systems for optimal heating and cooling [14], and reduction of peak energy demand in buildings [15]. In the study of energy efficient heating, Siroky et al. [16] carried out an experimental analysis of an MPC strategy using weather prediction approach. Over a two-month experiment modeled on a building in Prague, the Czech Republic, an energy saving of about 15% to 28% was achieved. Differences found in energy saving were due to the effect of various parameters, such as insulation level and variation in outside temperature. The results revealed a good consistency with the results of a large-scale simulation carried out in another study [17]. It is clear that MPC not only minimizes energy consumption, but also contributes to reduction in peak energy demand, which in turn can lower the operating costs of a building. Ma et al. [18] studied the effect of MPC strategy on reduction of peak electricity demand for cooling in a commercial building. Owing to the automatic off-peak pre-cooling effect and shifting of energy demand from peak to off-peak hours, the analysis using MPC resulted in a significant cost saving.

Other research has studied the role of MPC strategies in buildings using TES. For example, Zhao et al. [19] conducted an economic MPC-based study to optimize energy demand of a Hong Kong zero-carbon building. A stratified chilled water storage tank was integrated into the model as TES. The results showed reductions of 6–22% in energy consumption, 23–29% in operating costs, and 12–48% in CO_2 emissions, depending on the connection to grid and season of the year.

In fact, a considerable number of studies have applied MPC strategies to the HVAC systems of buildings to make them more energy-efficient [20]. The majority of this work has taken advantage of sensible thermal energy storage [21] to further improve energy savings. Much less work has been done on the incorporation of LHES into systems. In one example, Papachristou et al. [22] incorporated PCM into the fabrics of a building in Canada. The PCM was charged through forced air circulation in room. Their objective was to develop a low-order thermal network model for the design of MPC strategy as well as optimization of PCM performance. Finally, the comparison of the modeling results with experimental data showed a great match in predicting the peak power demand and room temperature profile. Touretzky and Baldea [23] embedded LHES into a chilled water tank energy storage system. Proposing a hierarchical control strategy, they tried to manage the cooling demand schema of building and enhance the operation of its electric grid. They investigated cost savings for different load leveling, which is a way to distribute power requirement more evenly during the day, to change the electricity demand patterns of building. As a result, a cost saving of about 88% was achieved for the higher load. It is worth noting that energy storage was the main element of load-leveling strategy. In this case, electricity was used to charge the water tank as well as the PCM with heat. However, utilizing solar energy would have been more advantageous. As the most abundant and free source of energy, solar energy has an enormous potential for heating and cooling of domestic and commercial buildings [24]. To take advantage of solar energy, Fiorentini et al. [25] performed an experimental study of a hybrid MPC strategy to mainly control the cooling process of a residential building in Australia. The building was modeled through a simple R-C model. For the sake of thermal energy management, they considered two hierarchical control modes for HVAC system; one with a 24-h prediction horizon and a 1-h control step, followed by a 1-h prediction horizon and a 5-min control step. Using an air-based photovoltaic thermal collector and a PCM storage, the controller was able

to satisfy the cooling demand of the room with a higher heat pump average coefficient of performance than the reference standard air conditioner.

To the authors' knowledge, economic MPC strategy has not been applied to buildings incorporating active PCM storage system charged by solar energy. In this content, a solar-assisted active HVAC system was controlled to minimize heating costs while providing the required comfortable temperature. This strategy was applied to domestic and service buildings and offices in winter, based on weather conditions of Auckland city in New Zealand. Considering the weather condition, the heating demand of buildings was calculated through EnergyPlus simulation, rather than using a simplified model. This data was saved in an excel interface, which then was called in Python to apply the MPC strategy. Fig. 1 gives an overview of the performance of MPC in the buildings of current study. In addition, the effect of some parameters such as receding horizon, decision time step, and mass capacity of PCM on energy costs, was studied.

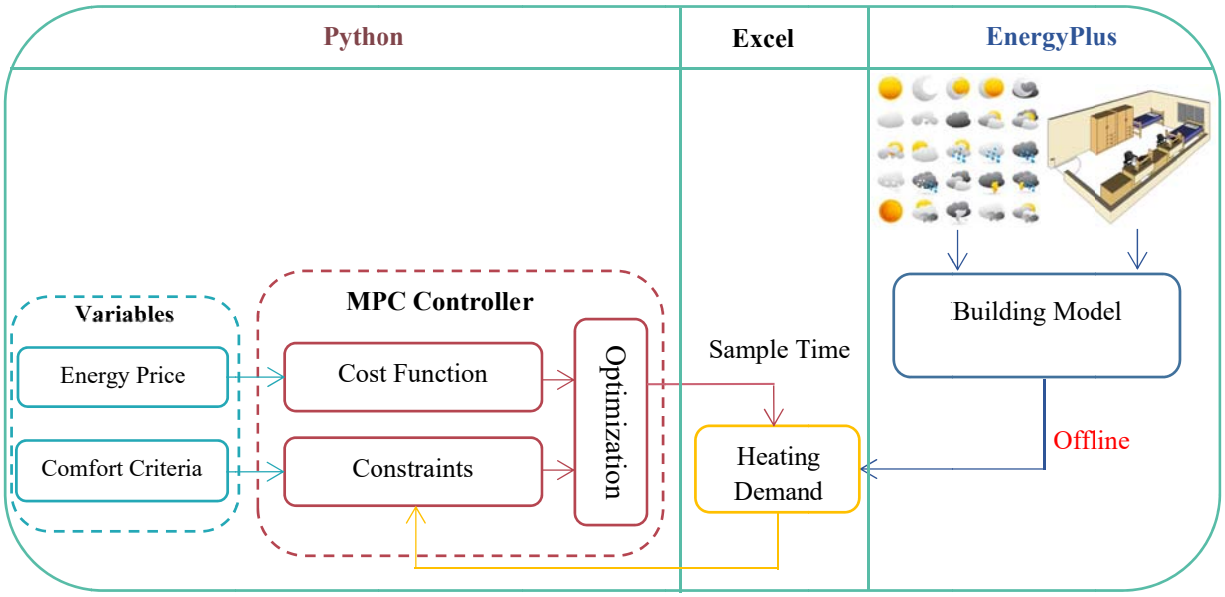

Fig. 1. Schematic view of the MPC controller performance in the building of current study

2. Methodology

2.1. Description of the system

2.1.1. General overview

Building automation systems are designed to control heating processes in service and domestic buildings, as well as offices. In this study, the building system comprised of a solar air collector, a heat exchanger filled with PCM, a backup heater, a fan to drive air from the heat exchanger to a standard basic building model (see more details in section 2.2), and energy to keep it at specific temperatures at specified times. The energy required to maintain thermal comfort of a standard basic building is termed '*demand*'. The heating demand of the standard room in this study could be supplied directly from the solar collector, the stored solar energy in the heat exchanger, and also from backup heater. There are three different operation modes for these energy sources, as described in the following paragraphs. By choosing the correct sequence for the operational modes, MPC can automatically provide a comfortable room temperature and reduce electricity cost.

Solar air collector mode: The solar collector mode is active when demand is coincident with the presence of sunlight. If solar energy is greater than demand, surplus thermal energy will be stored in the heat exchanger by charging PCM in it. In the event that the collected solar energy is greater than both demand and the energy required to charge PCM, the excess will be discharged into environment.

Heat exchanger discharge mode: Energy from PCM will be discharged if demand is greater than available energy from the solar collector. However, if at a given time the electricity rate is cheap, the optimizer tends to use backup heater and leave the PCM energy for hours of high electricity price.

Backup heater mode: If the heat exchanger and solar collector are not able to satisfy demand, the backup heater starts working. On the other hand, when the system is operating during hours of low cost electricity, even though solar energy is available or the heat exchanger is charged, MPC can decide to use the backup heater based on weather prediction.

In design of the system, the backup heater and heat exchanger were located inside the building. Thus, the energy loss from both maybe considered negligible. Fig. 2 shows an overview of automation system used in the current study.

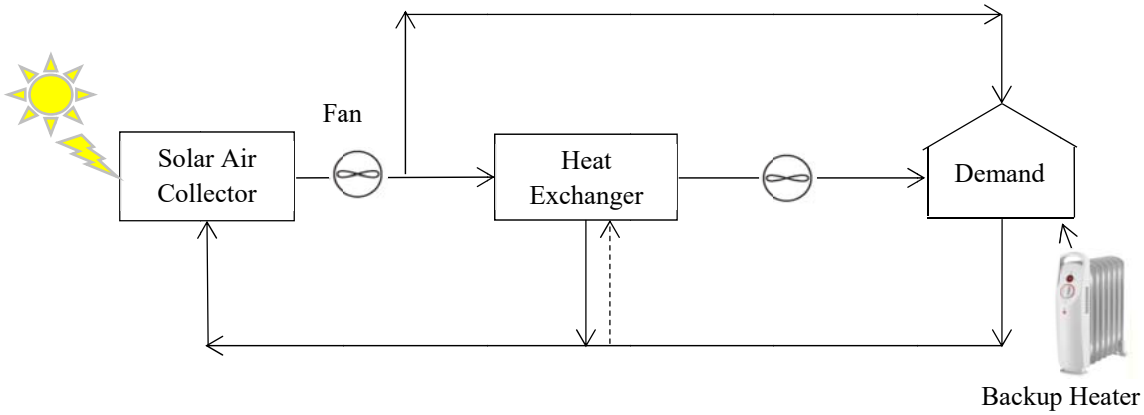

Fig. 2. Overview of the automation system

The aim of the automation system was to take advantage of low-cost nighttime electricity rates and diurnal solar energy, which in turn would culminate in reduction of global and peak energy demand, as well as energy costs. Being aware that the heating demand and energy consumption of a building can influence operational costs [26], a simulation-based optimization process was carried out to satisfy the MPC strategy (Section 2.4). Specifically, the heating demand of the building was evaluated through the simulation software (Section 2.2). Then, demand along with other input data will be sent to the optimizer (Section 2.3) to minimize heating cost of the building.

2.1.2. Solar air collector

Solar energy is the most available source of energy of all renewable and fossil-based energy resources [27]. Moreover, due to its clean, environmentally-friendly, and sustainable features, the application of solar energy has gained considerable attention [28]. Solar energy can be utilized using various technologies such as solar water heaters, solar cookers, solar dryers, solar ponds, solar architecture, solar air conditioning, and solar chimneys [29]. Hence, a fruitful and cost-effective approach is required to extract solar energy, convert it into thermal energy and then store it [30].

The focus of this study was on space heating of buildings. Therefore, a non-concentrating, flat plate solar collector was assumed as the source of energy. Flat plate collectors usually contain glass or plastic glazed covers, dark-colored absorber plates, insulation, tubes filled with a heat transfer fluid and other ancillaries [31]. The performance of a solar collector is evaluated by its efficiency, which is defined as the ratio of the useful thermal energy collected to the total amount of radiation hitting the surface of the collector over a specific period of time [32]. Assuming a constant value for some parameters, such as transmission coefficient of glazing, absorption coefficient of plate, collector heat removal factor, and collector overall heat loss coefficient, the efficiency will be a linear function of solar radiation intensity and the difference between inlet airflow of the collector and ambient temperature (Eq. (1)) [33]. This assumption is used to simplify working equations and the encoding process to accelerate the speed of the calculations.

$$\eta_{SAC} = 0.74 - 8.22\left(\frac{T_{in,SAC} - T_{amb}}{I}\right) \quad (1)$$

where, η is efficiency, T temperature, and I is the intensity of solar radiation. The subscript *SAC* is the acronym for the solar air collector. Subscripts *in* and *amb* represent the inlet and ambient temperature of the solar collector, respectively.

The collector in this study was a 1 m × 1 m solar air collector, incorporating a 0.1 m × 1 m photovoltaic (PV) panel on top of it (Fig. 3) to drive the fan needed to circulate the air through the collector. The efficiency of the solar collector was calculated using Eq. (1).

Fig. 3. Integrated solar collector and photovoltaic module

2.1.3. Heat exchanger

The heat exchanger unit in this study (Fig. 4) was made of acrylic materials and a set of 19 thin aluminum containers (0.45 m × 0.30 m × 0.01 m) holding a commercial PCM – RT25HC. The plates were positioned parallel to the airflow with 5mm gap between them. The heat exchanger unit was coupled with fan of the solar collector, or the fan used to drive air from heat exchanger to room allowing the circulation of air through the plates. The amount of PCM in the heat exchanger unit was approximately 9.5 kg. Table 1 details the

properties of PCM. The whole assembly was insulated using a 0.040 m thick layer of polystyrene and mineral wool (i.e. thermal resistance of about 1 $m^2 \cdot K/W$).

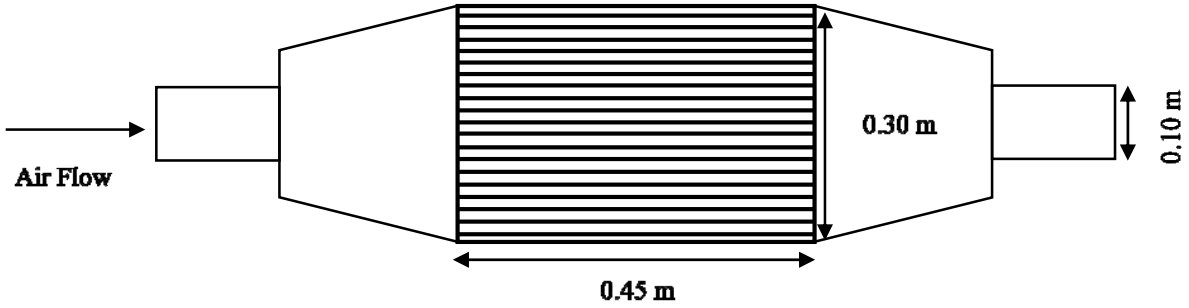

Fig. 4. Schematic top view of the heat exchanger

Table 1

The physical and thermal properties of the PCM –RT 25 HC [34].

Parameter	Unit	Value
PCM type	-	Organic
Melting temperature range	°C	22-26
Heat of fusion	kJ/kg	230
Specific heat	kJ/kg·K	2 (s)
		2 (l)
Thermal conductivity	W/m·K	0.2
Density	kg/m^3	880 (s)
		770 (l)
Volume expansion	%	12.5
Max operating temperature	°C	65

To evaluate the thermal behavior of the PCM, the specific heat capacity of the mushy phase was calculated using Eq. (2) [35].

$$C_{p,PCM}=\begin{cases} C_{p,s} & \mathrm{T}_{PCM}<\mathrm{T}_m-\dfrac{\Delta T_m}{2} \\ C_{p,s}+\dfrac{LH_{PCM}}{\Delta T_m} & \mathrm{T}_m-\dfrac{\Delta T_m}{2}<T_{PCM}<\mathrm{T}_m+\dfrac{\Delta T_m}{2} \\ C_{p,l} & \mathrm{T}_{PCM}>\mathrm{T}_m+\dfrac{\Delta T_m}{2} \end{cases} \quad (2)$$

where, C_p is specific heat capacity, LH is heat of fusion, and ΔT_m is an arbitrary small value representing the range of phase change temperature. Subscripts *s*, *l*, and *m* represent solid phase, liquid phase, and current and melting condition of PCM.

The findings rest on the assumption that all the PCM had same temperature [36]. Indeed, based on this isothermal model, de Gracia et al. [37] confirmed that discrepancies between the simplified model and the experimental data are negligible enough for engineers and architects to predict the performance of the LHES without the need for complicated computational resources. On the other hand, as the charging and discharging process of PCM are mainly driven by force convection, the heat losses and gains were only considered during the storage period. On this basis, the temperature of PCM at different time steps could be obtained from Eq. (3), meaning that PCM temperature at each time step was equal to the PCM temperature at previous time step, plus the energy earning from solar collector, minus the energy leaving the heat exchanger to the room.

$$T_{PCM(k+1)}=T_{PCM(k)}+\frac{\dot{Q}_{SAC-HE(k)}-\dot{Q}_{HE-Room(k)}}{M_{PCM}\times C_{p,PCM}}\times\Delta t \quad \text{Dynamics- state update} \quad (3)$$

$$\Delta t=t_{k+1}-t_k \quad (4)$$

where $\dot{Q}$ is the thermal power of the device, *k* is time step, Δt is the decision time step, and *M* is PCM mass. Subscripts *SAC-HE* and *HE-Room* represent energy from solar air collector to heat exchanger, and heat exchanger to room, respectively.

In order to facilitate the calculations, it was assumed that the outlet temperature of the heat exchanger was the linear function of PCM temperature (Eq. (5)) [38].

$$\varepsilon_{HE(k)} = \frac{T_{out,HE(k)} - T_{Room}}{T_{PCM(k)} - T_{Room}} \tag{5}$$

where subscript *out,HE* represents the outlet condition of heat exchanger.

2.1.4. Backup heater

Electric resistance heating is 100% efficient, as it converts nearly all the electrical energy to thermal energy. Hence, the electric power of heater is equal to the thermal power used to provide the heating demand [39]. To estimate the power of fan, Hastings [40] proposed Eq. (6).

$$\dot{Q}_f = \frac{\Delta p}{\eta_f} Q_{air} \tag{6}$$

where Δp is overall system pressure drop and Q is air volume flow rate. In this study $\frac{\Delta p}{\eta_f}$ was considered to be constant in order to simplify the problem and implement MPC strategy more simply.

2.2. Heating demand simulation

The simulation part of the study was performed via EnergyPlus v8.1. EnergyPlus is a powerful building energy simulation software, which is used widely by designers and engineers all over the world. This tool is able to estimate building energy demand according

to the envelope design, weather conditions, occupancy status, and HVAC system design and control [41]. EnergyPlus takes advantage of the features and capabilities of BLAST and DOE-2 programs, which have been supported by the US government, and builds new features such as variable time steps for HVAC simulation and user-configurable systems [42]. In fact, it is able to assess heat balance loads at fixed time steps, as well as the response of HVAC, plant and electrical systems at variable time steps. This integration has led to more precise and realistic temperature prediction, estimation of adsorption, desorption, radiant heating and cooling systems, advanced infiltration, and multi-zone airflow calculations [43].

In this study, ASHRAE standard 140 Case 600 was selected as the reference building to simulate the heating demand of three types of building through EnergyPlus software. According to this standard, the basic building model is a rectangular single zone with dimensions 8 m wide, 6 m long and 2.7 m high, and without any interior partitions. The building has two 12 m^2 windows, facing south (Fig. 5) [44]. However, as the current simulation was based on conditions in Auckland, New Zealand, a slight modification was carried on the test model to change the windows to north facing. The design of the standard building is based on lightweight construction materials. More information regarding the building specifications, such as envelope components and their properties, infiltration, internal loads and mechanical systems can be found in the publication cited in reference [44]. As ASHRAE standard was used to implement the reference building in EnergyPlus, no validation was done for simulation to calculate heating demand [45].

This study investigated the heating demand for different type of buildings, namely offices, and domestic and service buildings, each of which entailed its own schedule. The schedule represented the time of the day that the HVAC system needed to operate to maintain the space temperature at a specific range. Table 2 depicts the details of the schedules applied in simulation.

Table 2

The schedules of the service, office and domestic buildings [46].

Building	Comfort temperature range (°C)	Schedule time
Service	20-25	24 hour
Office	20-24	8 am – 4 pm
Domestic	20-24	6 pm – 12 am

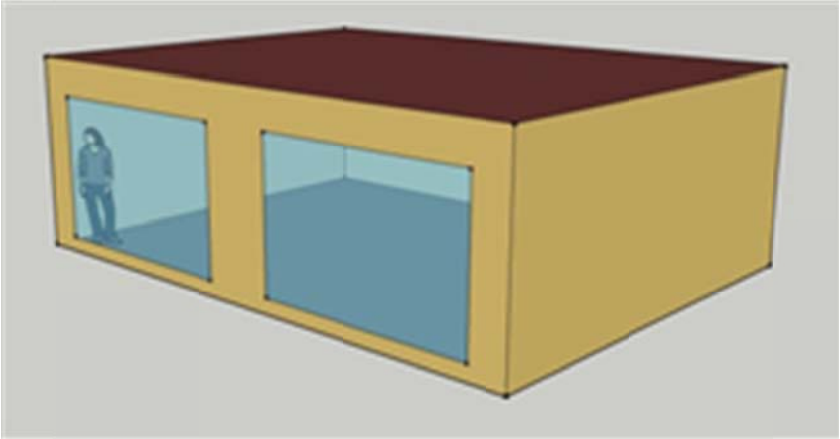

Fig. 5. ASHRAE Standard 140 Case 600

2.3. Numerical optimization

Solving Constraint Integer Programs (SCIP) Optimization Suite is a software toolbox, which can generate and solve algebraic optimization problems. Its modeling language is ZIMPL, the linear programming solver is SoPlex, and the constraint integer programming and branch-cut-and-price framework is SCIP. SCIP is able to quickly solve both mixed-integer linear and non-linear programming, MIP and MINLP. The other features of SCIP optimization Suite are UG frameworks used to parallelize branch-and-bound-based solvers, and GCG framework, which performs as a generic branch-cut-and-price solver [47].

As a well-defined and high-level programming interface, Python can be used to write SCIP codes [48]. Python is an outstanding tool, offering open-source, object-oriented, user-friendly, versatile, portable, extensible, and customizable software [49]. In addition, it has a standard library, which allows users to have access to a large number of useful modules, inter-process communication, and operating and file systems [50].

In this study, SCIP 4.0.0 as the optimizer and Python 2.7.12 as the programming interface, both of which were installed on an Ubuntu Linux operative system, were used to produce the dynamic model of system.

2.4. MPC strategy

An MPC tool is a successful optimization-based strategy, by which the behavior of a controlled system can be explicitly predicted over a receding horizon [51]. The main elements of MPC are objective function, prediction horizon, decision time step, manipulated variables, optimization algorithm, and feedback signals [52]. Along with its dynamic modeling of the process, MPC acts in a way to optimize the objective function, subject to some constraints [53]. The basic structure shown in Fig. **6** is used to implement the MPC strategy. In this strategy, a model is utilized to predict the outputs based on the past inputs and outputs and current inputs as well as the proposed optimal future control signals. These signals are calculated through the optimizer considering the objective function, constraints and future errors, for a determined horizon. The predicted output, then, is compared to reference trajectory and an error is calculated. The cycling process is continued until a minimal error is obtained [54].

In MPC strategy, Eq. (7) is used to introduce the objective function, and follows constraints required to satisfy the demand [16].

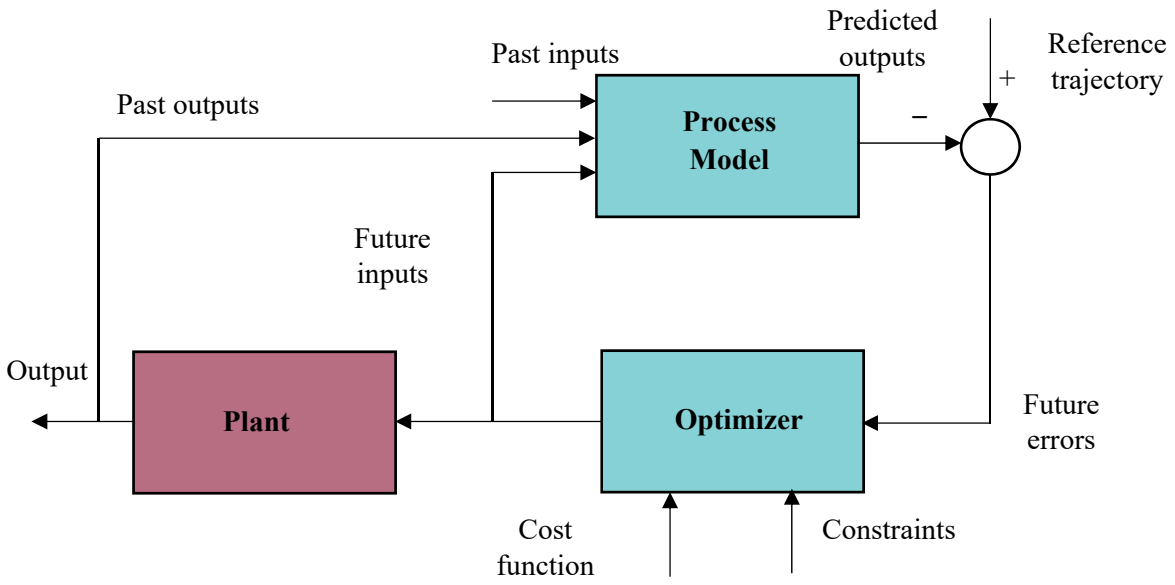

Fig. 6. Basic structure of MPC strategy [54]

$$\min_{u_0,\ldots,u_{N-1}} \sum_{k=0}^{N-1} l_k(x_k,u_k) \qquad \text{Objective function} \qquad (7)$$

subject to:

$$x_{k=0} = x_0 \qquad \text{Current state} \qquad (8)$$

$$x_{k+1} = f\left(x_k,u_k\right) \qquad \text{Dynamics- state update} \qquad (9)$$

$$\left(x_k,u_k\right) \in X_k \times U_k \qquad \text{Constraints} \qquad (10)$$

where, l is cost function, N is prediction horizon, $x_k \in \mathbb{R}^n$ is state, $u_k \in \mathbb{R}^m$ is control input, and X_k and U_k define the constraints of state and inputs values, respectively. In general, objective function should satisfy stability and target performance parameters. In fact, to prove its

stability, the objective function should be able to follow Lyapunov-like functions [55]. In terms of the target performance, the objective function usually needs to minimize one behavior and maximize another one [16]. For example the objective function of the current study tends to minimize the cost and maximize the inside thermal comfort.

The objective function used in this study (Eq. (11)) aimed to minimize the total energy cost of the heating, including the cost of backup heater and the fan applied to the system in order to drive air from TES to room at on-peak hours.

$$\text{Objective function: } \min_{\substack{\dot{Q}_{BH(0)},\ldots,\dot{Q}_{BH(N-1)} \\ \dot{Q}_{f(0)},\ldots,\dot{Q}_{f(N-1)}}} \sum_{k=0}^{N-1} (\dot{Q}_{BH(k)} + \dot{Q}_{f(k)}) \times \Delta t \times electricity\ price \tag{11}$$

subject to:

$$T_{PCM|k=0} = T_{PCM\,0} \qquad \text{Current state} \tag{12}$$

$$T_{PCM(k+1)} = T_{PCM(k)} + \frac{\dot{Q}_{SAC-HE(k)} - \dot{Q}_{HE-Room(k)}}{M_{PCM} \times C_{p,PCM}} \times \Delta t \qquad \text{Dynamic-state update} \tag{13}$$

$$Demand_{(k)} = \dot{Q}_{SAC-Room(k)} + \dot{Q}_{HE-Room(k)} + \dot{Q}_{BH(k)} \qquad \text{Constraint} \tag{14}$$

$$\dot{Q}_{SAC(k)} \geq \dot{Q}_{SAC-HE(k)} + \dot{Q}_{SAC-Room(k)} \qquad \text{Constraint} \tag{15}$$

$$\dot{m}_{SAC(k)} \geq \dot{m}_{SAC-HE(k)} + \dot{m}_{SAC-Room(k)} \qquad \text{Constraint} \tag{16}$$

$$\dot{m}_{SAC-Room(k)} = \frac{\dot{Q}_{SAC-Room(k)}}{C_{p,air}(T_{out,SAC} - T_{Room})} \qquad \text{Constraint} \tag{17}$$

$$\dot{m}_{SAC-HE(k)} = \frac{\dot{Q}_{SAC-HE(k)}}{C_{p,air}(T_{out,SAC} - T_{out,HE(k)})} \quad \text{Constraint} \quad (18)$$

$$\dot{m}_{HE-Room(k)} = \frac{\dot{Q}_{HE-Room(k)}}{C_{p,air}(T_{out,HE(k)} - T_{Room})} \quad \text{Constraint} \quad (19)$$

where $\dot{m}$ is mass flow rate and subscripts *f* and *SAC-Room* represent fan and solar collector to room, respectively. The subscript *PCM0* represents the initial condition of PCM. The operating range of variables is defined as below:

$$0 \leq \dot{m}_{SAC(k)} \ \& \ \dot{m}_{HE-Room(k)} \leq 0.2 \quad (20)$$

$$20 \leq T_{PCM(k)} \leq 60 \quad (21)$$

$$0 \leq \dot{Q}_{HE(k)} \ \& \ \dot{Q}_{BH(k)} \leq Maximum\ demand \quad (22)$$

$$0 \leq \dot{Q}_{SAC(k)} \leq Maximum\ energy\ from\ SAC \quad (23)$$

The energy cost obtained through MPC strategy was then compared with *'simple control'* method to estimate the cost savings for electrical energy. The basic idea of the simple control method is to compare the system output with the determined set point and minimize error by tuning process control inputs i.e. repeating a measurement and computation procedure for each time step. The simple control method fails to predict outputs as the horizon is ignored [56].

3. Results and discussion

3.1. Effect of receding horizon

One significant parameter in the evaluation of MPC performance is horizon [57]. The period of time in which the objective function is being optimized is called prediction horizon. In this section, results for the effect of MPC horizon on the heating costs of the aforementioned building types are discussed. Heating demand of a service building in a typical day of winter in Auckland was obtained through EnergyPlus simulation (Fig. 7). Fig. 8 displays the impact of receding horizon on electricity cost savings for service schedule profile for 1 and 7 running days, beginning with the first day of winter in Auckland in 2017. The cost savings achieved by the current strategy are compared with those with the simple control method. The decision time step of the figure is 15 min. Fig. 8 shows that increasing the horizon decreased the electricity consumption, which in turn resulted in a reduction in energy cost. Greater horizons enabled the model to cover a wider range of weather conditions as well as the electricity cost data, based on which the model decided whether to store or release the PCM energy to satisfy heating demand. In addition, it can be seen from the growth rate shown in the graphs that energy savings were more prominent when the duration of simulation increased from 1 to 7 days. This is because the model had more flexibility in relation to the charging and discharging time of the PCM. To clarify, in the 1-day (i.e. 24 h) simulation, heating demand resulting from the EnergyPlus simulation of the service schedule profile was for midnight until 9 am, and then from 8:30 pm to midnight (Fig. 7). Accordingly, PCM was only able to be charged during the day and discharged from 8:30 pm until midnight without causing any effect on the first period of demand. However, in the 7-day simulation, this period was extended, giving the PCM the ability to release its energy after second midnight and so save more energy.

In Fig. 8 the sharp increase shown in cost saving from 5 to 7.5 h is explained by Figs. 9 and 10, which exhibit the performance of MPC system for horizons 5 and 7.5 h, respectively. In these figures, electricity cost was extracted from reference [58] and solar radiation and demand were obtained from the simulation as input data. The PCM temperature and the sources of energies utilized to provide demand are the output information. Based on the first few winter days in Auckland, the most expensive time of the day was warm period, when there was no demand. At around 8 pm, demand started to grow, in which case for a system setting based on 5 h prediction (Fig. 9), it could use only a small proportion of solar energy (about 0.1 kW/m^2) stored in PCM. Hence, at 8:30 pm, a limited amount of energy could be released from the heat exchanger (red arrow). However, based on the 7.5 h prediction (Fig. 10), the system was able to take advantage of a larger amount of solar energy and release it at the time of need. Therefore, more energy savings and cost reductions were achieved.

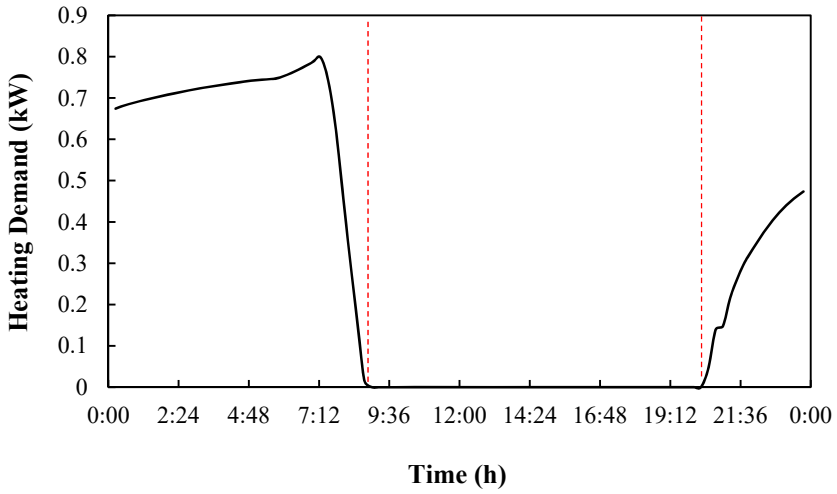

Fig. 7. The building heating demand in a 1-day simulation

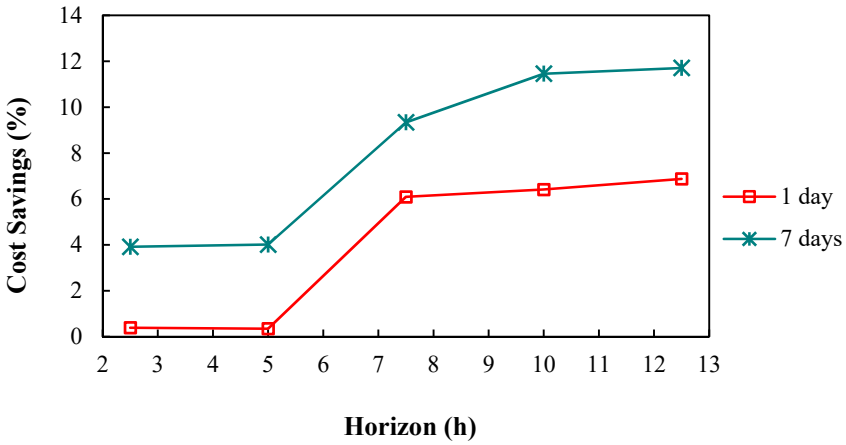

Fig. 8. Electricity cost savings at different horizons for 1 and 7 running days

The system decided to charge PCM based not only on the presence of the sun, but also on the conditions forecast. It can be observed that with the horizon of 5 h, the maximum temperature of PCM in heat exchanger was 23 °C. However, for a horizon of 7.5 h, it reached about 37 °C. In fact, with higher horizons, the system was able to anticipate a wider range of heating demand hours and store greater quantities of the solar energy in PCM. The results for 7 running days also confirm this finding (Fig. 11). Fig. 11 shows the behavior of the PCM's temperature at different horizons of 5, 7.5 and 10 h for 7 days, for given solar radiation, electricity cost and building heating demand. The trends show that with horizons ascending from 5 to 7.5 and 10 h, the maximum temperature of PCM, as well as retention time at that temperature, rose. Indeed, according to the prediction for 5 h, the system was exposed to demand when solar energy was not available. Thus, PCM remained unloaded. In contrast, applying the 10 h prediction allowed the PCM to be charged at a higher temperature, and for a longer time.

Further, the MPC strategy performed in such a way that the electricity and energy stored in the heat exchanger were consumed during the corresponding cheap and costly hours,

respectively. According to Figs. 9 and 10, at around 8 am there was a PCM discharge, even though the electricity cost was quite cheap (blue arrow). This is because at that time, with horizons of 5 and 7.5 h, no demand was foreseen. Thus, the MPC system attempted to extract the energy from heat exchanger during cheap hours, to avoid using backup heater energy and minimize the cost.

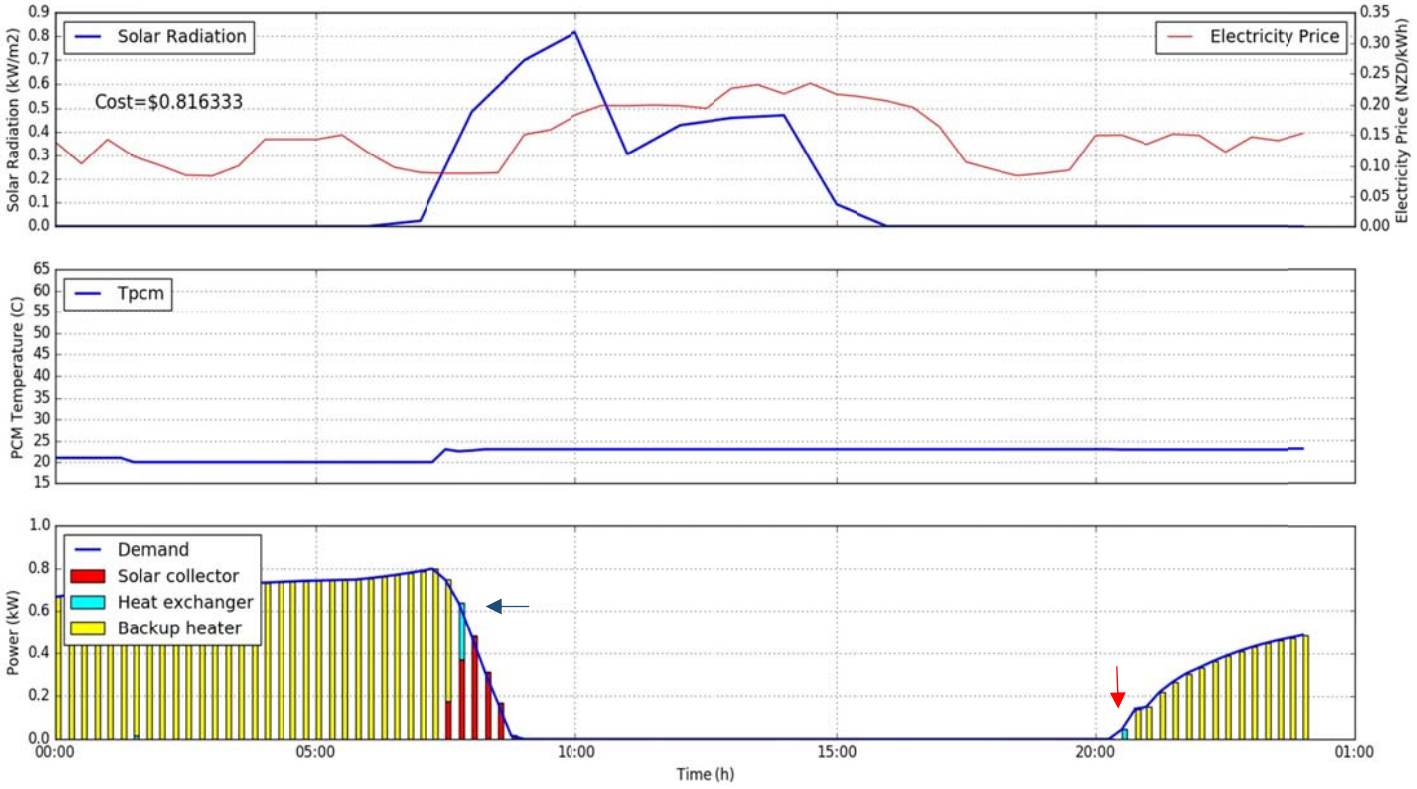

Fig. 9. The performance of the MPC with the horizon of 5 h for 1 day

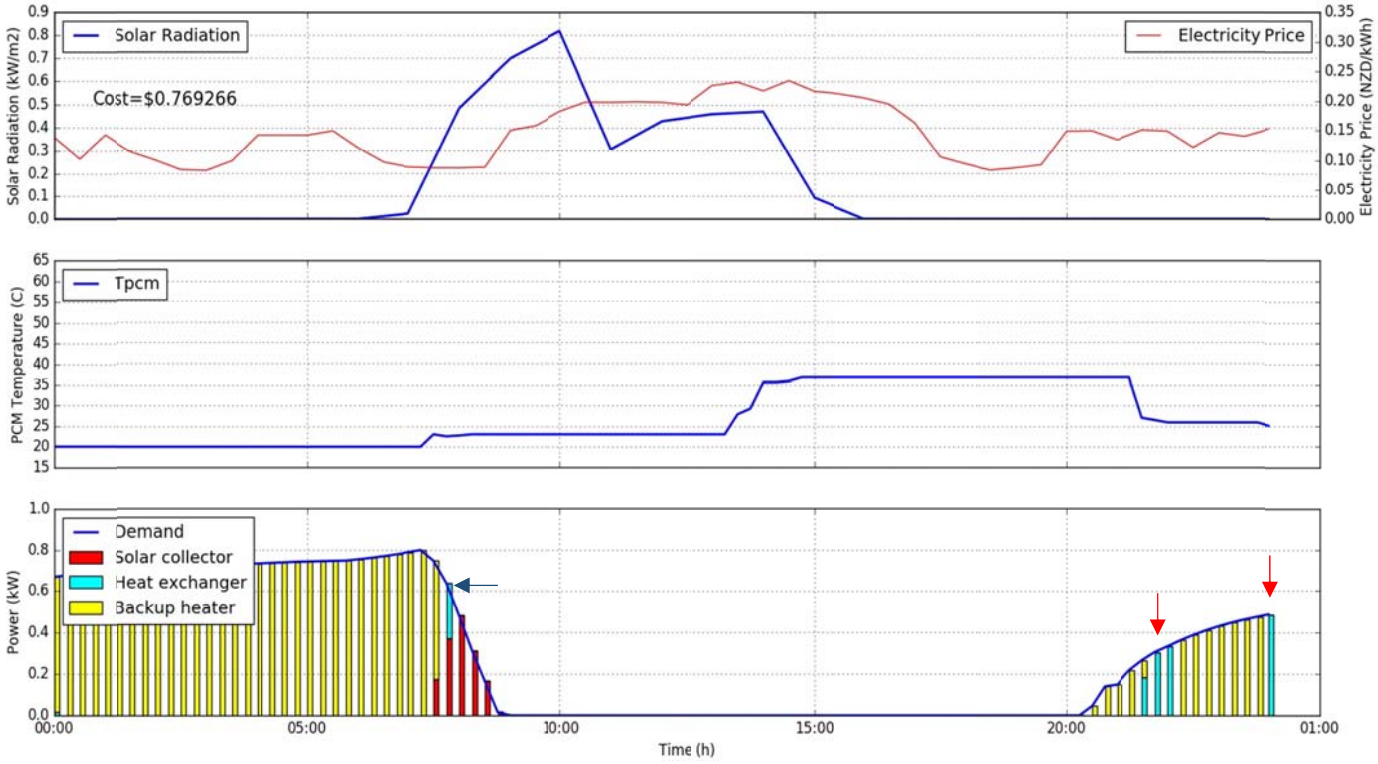

Fig. 10. The performance of the MPC with the horizon of 7.5 h for 1 day

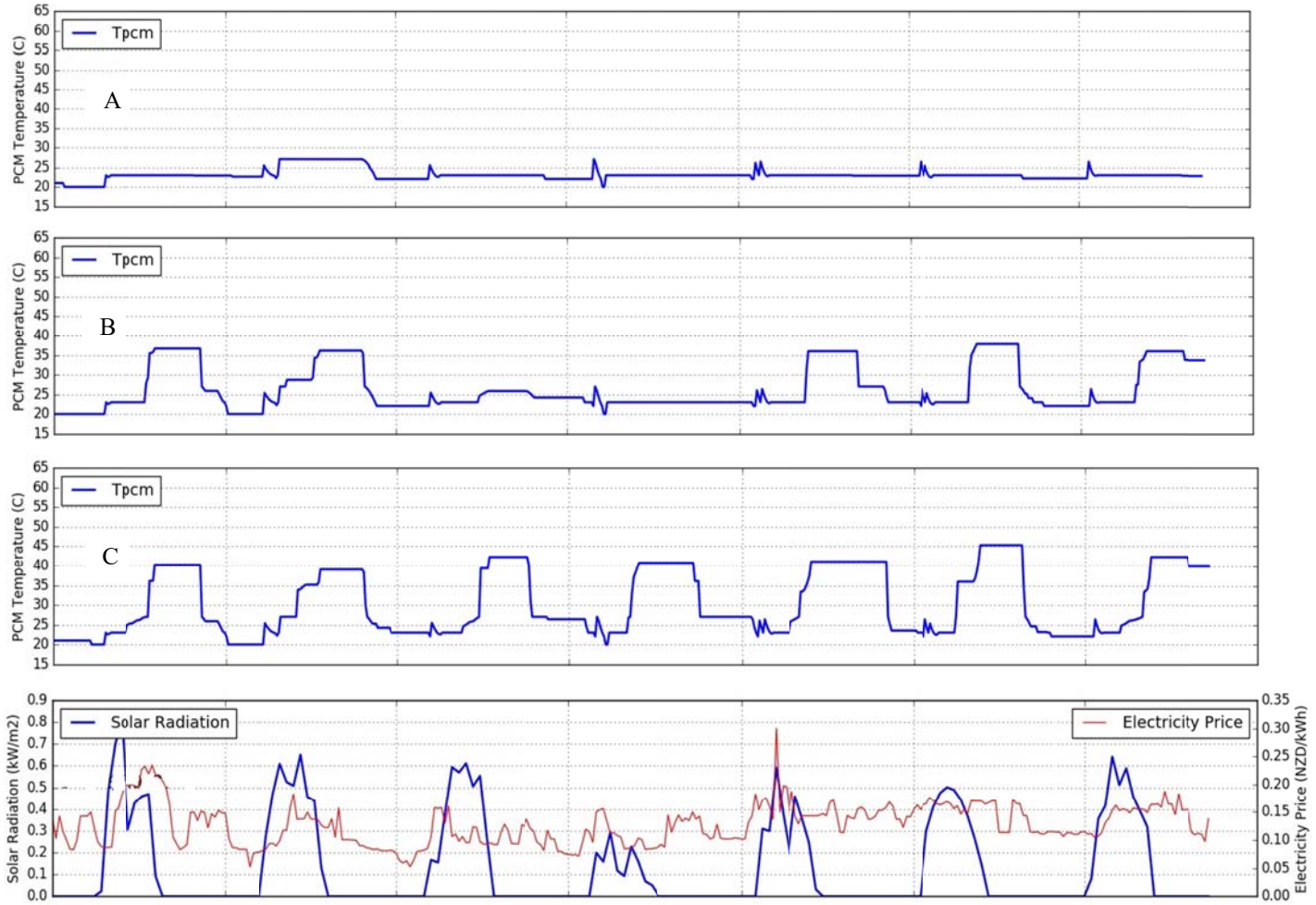

Fig. 11. The PCM temperature profile at horizons of A) 5 h, B) 7.5 h and C) 10 h for 7 days

3.2. Effect of decision time step

The duration between each optimization process is known as decision time step. Some researchers have studied the impact of decision time step on the performance of MPC strategies [59]. Table 3 presents the electricity cost of heating as a function of decision time step for the first 1 and 7 days of winter in Auckland. As shown in the table, for a specific number of horizons (i.e. 24 in this study), the longest decision time step appeared to be more efficient. Indeed, according to the relation between the horizon and decision time step (Eq. (24)), lengthening the decision time step expanded the prediction hours, which in turn culminated in reducing the energy consumption.

$$\text{Receeding horizon } (h) = N \times \Delta t \ (h) \tag{24}$$

However, the accuracy of system is another critical parameter that should be taken into account. While less complicated and time-consuming, large decision time steps may lead to some important data being missed, hence deteriorating the precision of the outcome. In this case, the reduction rate of the electricity cost for 7 days was less than for 1 day (Fig. 12). Based on the discussion in Section 3.1, an opposite scenario was expected. In the 7-day simulation, almost the same cost savings were achieved for both 30 and 60 min decision time steps, even though the prediction time of the latter is two times that of the former. In fact, due to skipping some essential information such as demand, weather condition, electricity cost, and PCM temperature, the system failed to provide an authentic estimation of energy and cost requirement. In other words, for the decision time step of 60 min, PCM reached its maximum point quickly, so that no further improvement was attained. This conclusion is verified by PCM temperature profile in Fig. 13, which indicates that PCM temperature oscillated sharply

between the boundaries temperatures of the program (20 and 60 °C) with 60 min decision time step. The temperature variation was more gradual with the 30 min time step, indicating it is better to make the time step as small as possible. However, as discussed, decreasing the time steps increases the time and cost of computations. On the other hand, longer time steps make the system more sensitive to sharp changes, meaning a contingency plan has to be developed to avoid malfunctioning of the system, such as not meeting demand and overheating PCM in the heat exchanger unit. Hence, a balance between the cost and accuracy of the program needs to be established.

Table 3

The energy cost of heating for 1 and 7 day simulations at different decision time steps

Decision time step (min)	Horizon (h)	Energy cost (NZD) for 1 day	Energy cost (NZD) for 7 days
5	2	0.802	7.205
15	6	0.790	6.350
30	12	0.750	5.795
60	24	0.660	5.760

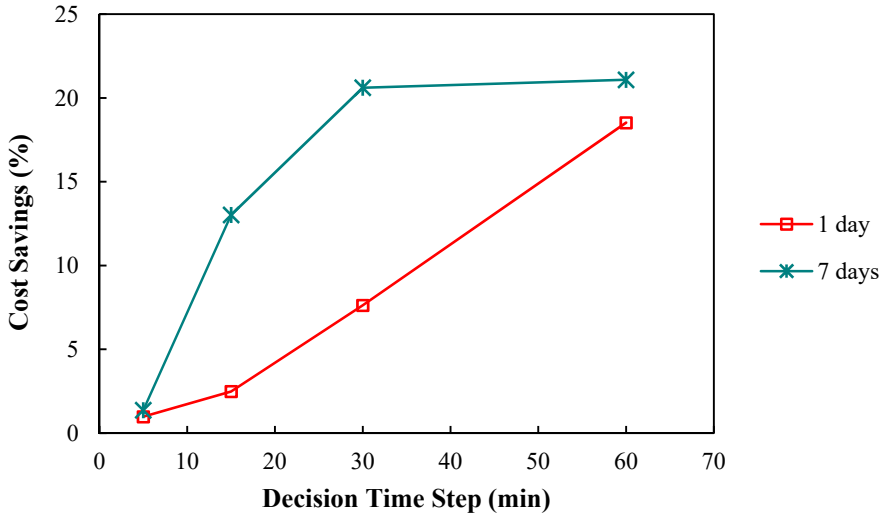

Fig. 12. Electricity cost savings at different decision time steps for 1 and 7 running days

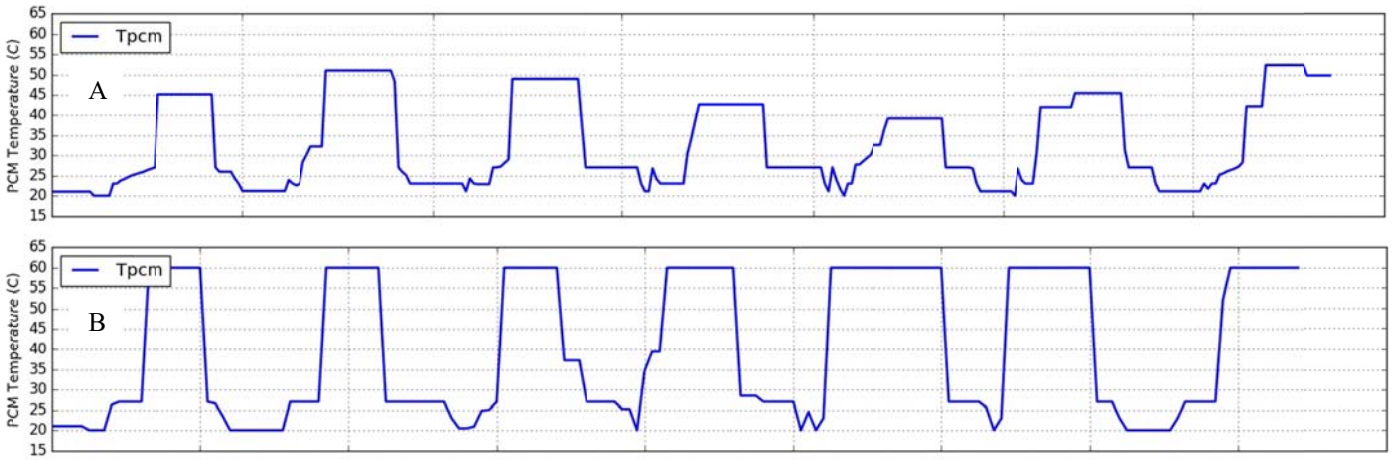

Fig. 13. PCM temperature profile for decision time steps of (A) 30 min and(B) 60 min, at given solar radiation and electricity cost

3.3. Effect of mass capacity of PCM

As a latent heat storage medium, PCM plays a significant role in the heating process of a space. In order to exploit the maximum efficiency of PCM, investigation of effective parameters of PCM performance was seen as beneficial. Accordingly, the objective in this part of the study was to demonstrate the impact of the amount of PCM in the heat exchanger on energy saving of the described service building, for 1 and 7 running days. The decision time step and horizon were considered to be 0.5 and 15 h, respectively. As expected, Fig. 14 shows that increasing the PCM mass helped the system to store more solar energy. Accordingly, the heat exchanger was able to release a greater amount of energy, leading to more electrical energy being saved. Applying 28.5 kg of PCM (three times the initial PCM) into the system saved about 27% in electricity costs in 7 days, which would provide remarkable savings over the whole winter, as well as over a couple of years in a row. However, it is not a good idea to raise the amount of PCM as much as possible. Instead, the PCM mass implemented in the heat exchanger should be optimized according to the efficiency of unit, as well as the capital investment of PCM.

In contrast to the 7-day simulation, increasing the amount of PCM from 19 to 28.5 kg in the1-day simulation did not improve the efficiency of the system. The reason is that at the given prediction horizon and decision time step, almost all the heating demand of the period between 8:30 pm and midnight was satisfied by the stored energy of the PCM (Fig. 15). Hence, further addition of PCM was not effective.

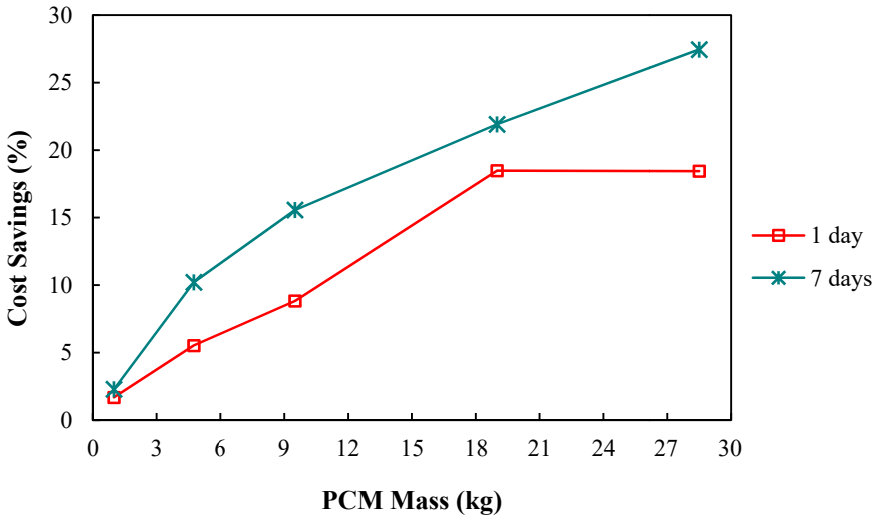

Fig. 14. Effect of PCM mass on the electricity cost savings for 1 and 7 running days

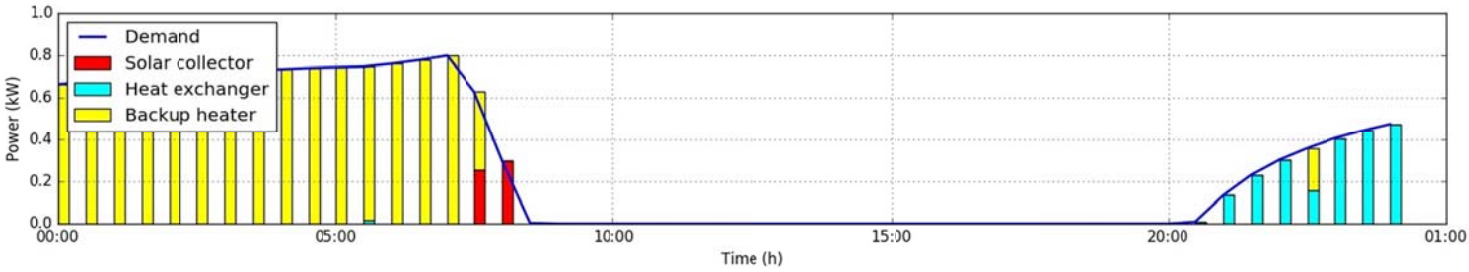

Fig. 15. The performance of the MPC system with 19 kg of PCM and horizon of 15 h

3.4. MPC performance in different buildings

MPC strategies can be applied to different type of buildings with different heating demands. Fig. 16 displays the heating demand for service, domestic, and office building scenarios, as well as energy sources used to supply the demand. In this simulation, decision time step and horizon are 0.25 and 10 h, respectively. The results of the simulation are compatible with the schedules for the buildings outlined in Table 2. The plan for service building was to maintain comfort zone over a 24-hour period. Hence, demand was zero only when solar energy was available to warm up the space. In this case, according to the available energy sources, the heat exchanger provided a small proportion of demand, while backup heater supplied a large proportion. Domestic buildings only need to be kept within specified range from 6 pm until midnight. Therefore, the energy stored in PCM during the day can largely meet demand. For the case of office building in this study, demand appeared particularly high during the day, and could be mostly met by solar energy, or energy stored in the heat exchanger. Thus, MPC strategy performed more effectively for office and domestic buildings than for service building in this study. Confirming the results, the 7-day simulation for different building types (Fig. 17) also showed the highest cost saving (56%) for domestic building, where a large amount of the heating demand was satisfied by discharging the PCM. The service building showed the lowest cost saving, as they should provide the comfortable indoor temperature for 24 hour.

Furthermore, when demand was compared in the 7-day simulation (Fig. 18), the intensity of demand in office building was larger than for the domestic building, which in turn showed greater intensity of demand than the service building. The reason for this is associated with the period of demand for each building. In the office building, demand rose after the low temperature at night, which made the building very cold, meaning it needed more energy than the other buildings to compensate. In contrast, the demand intensity for the domestic

buildings was the lowest as it appeared at around 8 pm, after taking advantage of daytime sunlight and warm temperatures. Finally, the demand intensity for the service building was between that of the two buildings. It needed to be considered all the time, so the building's temperature did not get too low.

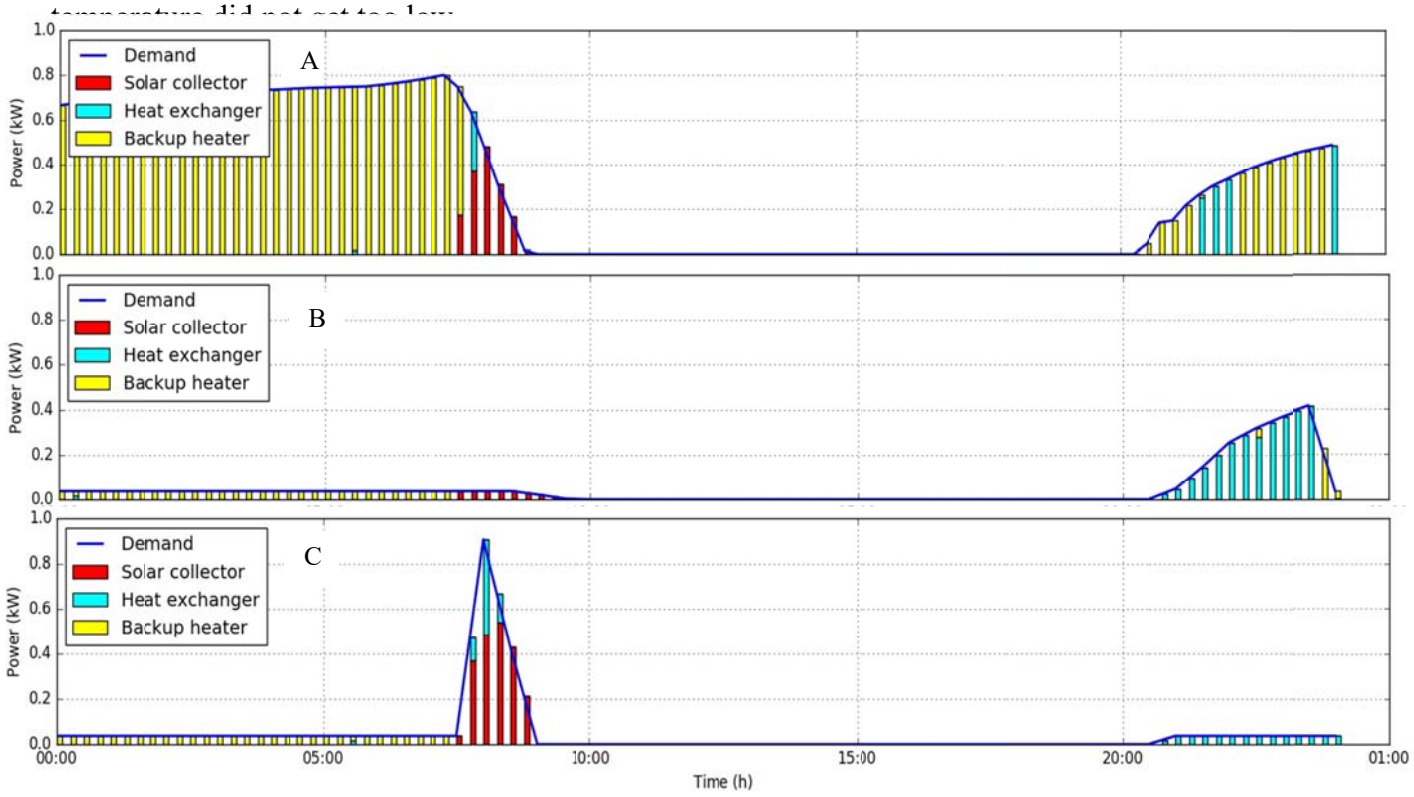

Fig. 16. The profile demand and the sources of energy used to supply the demand for A) service, B) domestic and C) office buildings

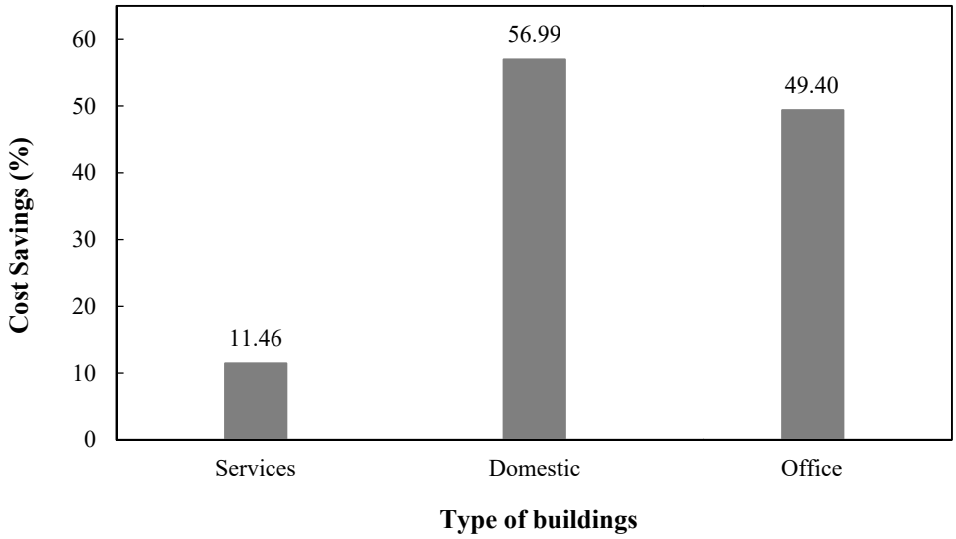

Fig. 17. Cost savings achieved by different type of building for the 7-day simulation

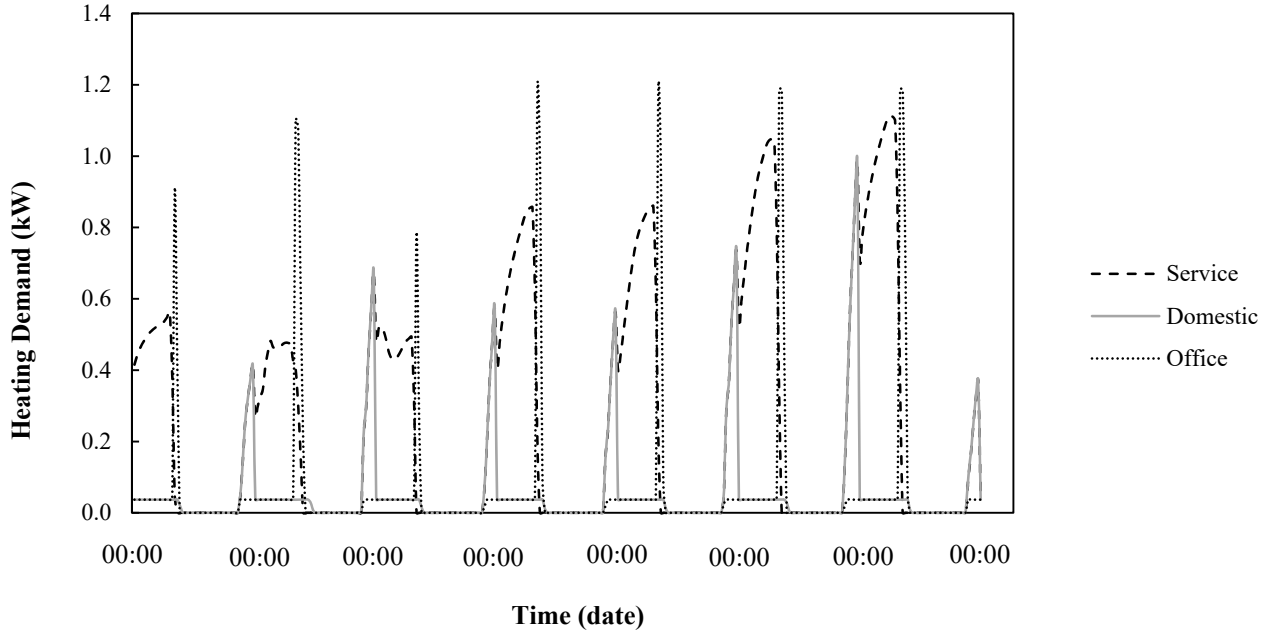

Fig. 18. Heating demand associated with different buildings

The summary of the investigated parameters, operating conditions and schedules as well as the findings of the current study are shown in Table 4. In fact, the effect of horizon, decision time step, PCM mass and operating schedule on cost savings of heating process of a building in New Zealand were studied.

Table 4

Summary of the operating conditions and findings

Parameter	Horizon numbers	Decision time step (min)	PCM Mass (kg)	Simulation time (day)	Schedule	Cost savings (%)
Horizon	10, 20, 30	15	9.50	1	Service	0.34–6.80

numbers				7		4–11.70
Decision time step	24	5, 15, 30, 60	9.50	1 7	Service	0.97–18.50 1.37–21.10
PCM Mass	30	30	1, 4.75, 9.50, 19, 28.50	1 7	Service	1.69– 18.45 2.29–27.45
Schedule	40	15	9.50	7	Service Domestic Office	11.46 56.99 49.40

Conclusions

A numerical study was carried out of an MPC strategy to control the heating process for three versions of a standard building, all equipped with a heat exchanger containing PCM and a solar air collector to capture the solar energy and direct it to the heat exchanger. In this simulation-based optimization investigation, EnergyPlus, Python and SCIP software packages were used as the simulator, interface and optimizer, respectively. The objective function of the MPC was to select the appropriate schedule of operation for the whole system to minimize the electricity cost and meet the heating demand of the service, domestic, and office buildings used in the simulation. The results confirmed that implementation of the smart MPC strategy was more beneficial for the service building, followed by the office and domestic buildings in descending order. The effect of various parameters on the performance of the MPC strategy was investigated. The results showed that the greater the prediction horizon, the higher the cost saving achieved. Moreover, increasing the time step enhanced the horizon hours on the one hand, but ignored some significant input information on the other. Thus, smaller time steps were better in terms of the accuracy of the simulation. However, using smaller time steps requires more processing time and more powerful instruments, which increases the cost of computations. In addition, with regard to the PCM content of the

heat exchanger, a higher amount was more beneficial in terms of cost savings for electricity. However, increases in the capital cost of PCM would necessitate deciding on an optimized amount of PCM for the heat exchanger. Overall, the results show that compared to the simple control method, a cost saving of about 12 to 27% was achieved in the 7-day simulation in the domestic building, which was higher than for the 1-day simulation.

Acknowledgements

The study was partially funded by the Spanish Government (ENE2015-64117-C5-1-R (MINECO/FEDER) and ENE2015-64117-C5-3-R (MINECO/FEDER)). The authors at the University of Lleida would like to thank the Catalan Government for the quality accreditation given to their research group (2017 SGR 1537). GREiA is the certified agent for TECNIO in the category technology developers for the Government of Catalonia. The research leading to these results also received funding from the European Union's Seventh Framework Programme (FP7/2007-2013) under grant agreement no. PIRSES-GA-2013-610692 (INNOSTORAGE).

References

[1] Barzin R, Chen JJJ, Young BR, Farid MM. Application of PCM energy storage in combination with night ventilation for space cooling. Appl Energy 2015;158:412–21. doi:10.1016/j.apenergy.2015.08.088.

[2] Nejat P, Jomehzadeh F, Taheri MM, Gohari M, Muhd MZ. A global review of energy consumption, CO_2 emissions and policy in the residential sector (with an overview of the top ten CO_2 emitting countries). Renew Sustain Energy Rev 2015;43:843–62.

doi:10.1016/j.rser.2014.11.066.

[3] Kirubakaran V, Sahu C, Radhakrishnan TK, Sivakumaran N. Energy efficient model based algorithm for control of building HVAC systems. Ecotoxicol Environ Saf 2015;121:236–43. doi:10.1016/j.ecoenv.2015.03.027.

[4] Zhou D, Zhao CY, Tian Y. Review on thermal energy storage with phase change materials (PCMs) in building applications. Appl Energy 2012;92:593–605. doi:10.1016/j.apenergy.2011.08.025.

[5] Hien WN, Poh LK, Feriadi H. Computer-Based Performance Simulation for Building Design and Evaluation: The Singapore Perspective. Simul Gaming 2003;34:457–77. doi:10.1177/1046878103255917.

[6] Couenne F, Hamroun B, Jallut C. Experimental investigation of the dynamic behavior of a large-scale refrigeration e PCM energy storage system . Validation of a complete model. Energy 2016;116:32–42. doi:10.1016/j.energy.2016.09.098.

[7] Prívara S, Cigler J, Váňa Z, Oldewurtel F, Sagerschnig C, Žáčeková E. Building modeling as a crucial part for building predictive control. Energy Build 2013;56:8–22. doi:10.1016/j.enbuild.2012.10.024.

[8] Ebrahimpour M, Santoro BF. Moving horizon estimation of lumped load and occupancy in smart buildings. 2016 IEEE Conf Control Appl 2016:468–73. doi:10.1109/CCA.2016.7587874.

[9] Killian M, Kozek M. Ten questions concerning model predictive control for energy efficient buildings. Build Environ 2016;105:403–12. doi:10.1016/j.buildenv.2016.05.034.

[10] Braun JE. Load Control Using Building Thermal Mass. J Sol Energy Eng 2003;125:292–301. doi:10.1115/1.1592184.

[11] Carrascal-Lekunberri E, Garrido I, Van Der Heijde B, Garrido AJ, Sala JM, Helsen L. Energy conservation in an office building using an enhanced blind system control. Energies 2017;10. doi:10.3390/en10020196.

[12] Ma Y, Borrelli F, Hencey B, Packard A, Bortoff S. Model Predictive Control of thermal energy storage in building cooling systems. Proc 48h IEEE Conf Decis Control Held Jointly with 2009 28th Chinese Control Conf 2009:392–7. doi:10.1109/CDC.2009.5400677.

[13] Moroşan P-D, Bourdais R, Dumur D, Buisson J. Building temperature regulation using a distributed model predictive control. Energy Build 2010;42:1445–52. doi:10.1016/j.enbuild.2010.03.014.

[14] Yudong M, Matusko J, Borrelli F. Stochastic Model Predictive Control for Building HVAC Systems: Complexity and Conservatism. Control Syst Technol IEEE Trans 2015;23:101–16. doi:10.1109/TCST.2014.2313736.

[15] Oldewurtel F, Ulbig A, Parisio A, Andersson G, Morari M, Ieee. Reducing Peak Electricity Demand in Building Climate Control using Real-Time Pricing and Model Predictive Control. 49th Ieee Conf Decis Control 2010:1927–32. doi:10.1109/cdc.2010.5717458.

[16] Široký J, Oldewurtel F, Cigler J, Prívara S. Experimental analysis of model predictive control for an energy efficient building heating system. Appl Energy 2011;88:3079–87. doi:10.1016/j.apenergy.2011.03.009.

[17] Gyalistras D, Fischlin A, Zurich E, Morari M, Jones CN, Oldewurtel F, et al. Use of Weather and Occupancy Forecasts for Optimal Building Climate Control Facts of the project. vol. 41. 2010.

[18] Ma J, Qin J, Salsbury T, Xu P. Demand reduction in building energy systems based on

economic model predictive control. Chem Eng Sci 2012;67:92–100. doi:10.1016/j.ces.2011.07.052.

[19] Zhao Y, Lu Y, Yan C, Wang S. MPC-based optimal scheduling of grid-connected low energy buildings with thermal energy storages. Energy Build 2015;86:415–26. doi:10.1016/j.enbuild.2014.10.019.

[20] Knudsen MD, Petersen S. Model predictive control for demand response of domestic hot water preparation in ultra-low temperature district heating systems. Energy Build 2017;146:55–64. doi:10.1016/j.enbuild.2017.04.023.

[21] Labidi M, Eynard J, Faugeroux O, Grieu S. A new strategy based on power demand forecasting to the management of multi-energy district boilers equipped with hot water tanks. Appl Therm Eng 2017;113:1366–80. doi:10.1016/j.applthermaleng.2016.11.151.

[22] Papachristou AC, Vallianos CA, Dermardiros V, Athienitis AK, Candanedo JA. A numerical and experimental study of a simple model-based predictive control strategy in a perimeter zone with phase change material. Sci Technol Built Environ 2018;4731. doi:10.1080/23744731.2018.1438011.

[23] Touretzky CR, Baldea M. A hierarchical scheduling and control strategy for thermal energy storage systems. Energy Build 2016;110:94–107. doi:10.1016/j.enbuild.2015.09.049.

[24] Hawlader MNA, Uddin MS, Khin MM. Microencapsulated PCM thermal-energy storage system. Appl Energy 2003;74:195–202. doi:10.1016/S0306-2619(02)00146-0.

[25] Fiorentini M, Wall J, Ma Z, Braslavsky JH, Cooper P. Hybrid model predictive control of a residential HVAC system with on-site thermal energy generation and storage. Appl Energy 2017;187:465–79. doi:10.1016/j.apenergy.2016.11.041.

[26] Fumo N, Mago P, Luck R. Methodology to estimate building energy consumption using EnergyPlus Benchmark Models. Energy Build 2010;42:2331–7. doi:10.1016/j.enbuild.2010.07.027.

[27] Lewis NS. Toward Cost-Effective Solar energy use. Science (80-) 2007;315:798–802.

[28] Panwar NL, Kaushik SC, Kothari S. Role of renewable energy sources in environmental protection: A review. Renew Sustain Energy Rev 2011;15:1513–24. doi:10.1016/j.rser.2010.11.037.

[29] Thirugnanasambandam M, Iniyan S, Goic R. A review of solar thermal technologies. Renew Sustain Energy Rev 2010;14:312–22. doi:10.1016/j.rser.2009.07.014.

[30] Mekhilef S, Saidur R, Safari A. A review on solar energy use in industries. Renew Sustain Energy Rev 2011;15:1777–90. doi:10.1016/j.rser.2010.12.018.

[31] Tian Y, Zhao CY. A review of solar collectors and thermal energy storage in solar thermal applications. Appl Energy 2013;104:538–53. doi:10.1016/j.apenergy.2012.11.051.

[32] Chabane F, Moummi N, Benramache S, Bensahal D, Belahssen O. Collector efficiency by single pass of solar air heaters with and without using fins. Eng J 2013;17:43–55. doi:10.4186/ej.2013.17.3.43.

[33] Struckmann F. Analysis of a Flat-Plate Solar Collector. 2008. doi:10.3846/mla.2011.108.

[34] Rubitherm Technologies GmbH. Macroencapsulation - CSM n.d. https://www.rubitherm.eu/en/index.php/productcategory/makroverkaspelung-csm (accessed March 1, 2018).

[35] Promoppatum P, Yao S, Hultz T, Agee D. Experimental and numerical investigation of the cross-flow PCM heat exchanger for the energy saving of building HVAC. Energy

Build 2017;138:468–78. doi:10.1016/j.enbuild.2016.12.043.

[36] Hed G, Bellander R. Mathematical modelling of PCM air heat exchanger. Energy Build 2006;38:82–9. doi:10.1016/j.enbuild.2005.04.002.

[37] De Gracia a., Castell a., Fernández C, Cabeza LF. A simple model to predict the thermal performance of a ventilated facade with phase change materials. Energy Build 2015;93:137–42. doi:10.1016/j.enbuild.2015.01.069.

[38] Cengel Y a. HEAT TRANSFER: A Practical Approach. Second. New York: McGraw-Hill; 2003.

[39] Energy Saver. Electric Resistance Heating. US Dep Energy 2016. https://energy.gov/energysaver/electric-resistance-heating (accessed March 1, 2018).

[40] Hastings R. Solar air systems: a design handbook. New York: Routledge; 2013.

[41] Stadler M, Firestone R, Curtil D, Marnay C, Berkeley L. On-Site Generation Simulation with EnergyPlus for Commercial Buildings. Buildings 2006:242–54.

[42] Crawley DB, Lawrie LK, Winkelmann FC, Buhl WF, Huang YJ, Pedersen CO, et al. EnergyPlus: Creating a new-generation building energy simulation program. Energy Build 2001;33:319–31. doi:10.1016/S0378-7788(00)00114-6.

[43] Crawley DB, Hand JW, Kummert M, Griffith BT. Contrasting the capabilities of building energy performance simulation programs. Build Environ 2008;43:661–73. doi:10.1016/J.BUILDENV.2006.10.027.

[44] Henninger R, Witte M. EnergyPlus testing with building thermal envelope and fabric load tests from ANSI/ASHRAE Standard 140-2007. 2014.

[45] Saffari M, de Gracia A, Fernández C, Cabeza LF. Simulation-based optimization of PCM melting temperature to improve the energy performance in buildings. Appl

Energy 2017;202:420–34. doi:10.1016/j.apenergy.2017.05.107.

[46] CEN (European Committee for Standardization). Indoor environmental input parameters for design and assessment of energy performance of buildings addressing indoor air quality, thermal environment, lighting and acoustics. 2007. doi:10.1520/E2019-03R13.

[47] Gamrath G, Fischer T, Gally T, Gleixner AM, Hendel G, Koch T, et al. The scip optimization suite 3.2. ZIB Rep 2016;60:15–60.

[48] Ferreto TC, Netto M a. S, Calheiros RN, De Rose C a. F. Server consolidation with migration control for virtualized data centers. Futur Gener Comput Syst 2011;27:1027–34. doi:10.1016/j.future.2011.04.016.

[49] Hart WE, Watson JP, Woodruff DL. Pyomo: Modeling and solving mathematical programs in Python. Math Program Comput 2011;3:219–60. doi:10.1007/s12532-011-0026-8.

[50] Prechelt L. Are Scripting Languages Any Good? A Validation of Perl, Python, Rexx, and Tcl against C, C++, and Java. Adv Comput 2003;57:205–70. doi:10.1016/S0065-2458(03)57005-X.

[51] Rao C, Rawlings J. Linear Programming and Model Predictive Control. J Process Control 2000;10:283–9.

[52] Thieblemont H, Haghighat F, Ooka R, Moreau A. Predictive control strategies based on weather forecast in buildings with energy storage system: A review of the state-of-the art. Energy Build 2017;153:485–500. doi:10.1016/j.enbuild.2017.08.010.

[53] Prívara S, Široký J, Ferkl L, Cigler J. Model predictive control of a building heating system: The first experience. Energy Build 2011;43:564–72. doi:10.1016/j.enbuild.2010.10.022.

[54] Camacho EF, Bordons C. Model Predictive Control. 2007. doi:10.1007/978-0-85729-398-5.

[55] Ellis M, Christofides PD. Performance Monitoring of Economic Model Predictive Control Systems. Ind Eng Chem Res 2014;53:15406–13. doi:10.1021/ie403462y.

[56] Åström KJ, Hägglund T. The future of PID control. Control Eng Pract 2001;9:1163–75. doi:10.1016/S0967-0661(01)00062-4.

[57] Kummert M, André P, Nicolas J. Building and HVAC Optimal Control Simulation. Application to an Office Building. Proc Third Int Symp HVAC 1999:857–68.

[58] Electricity Authority. NZX Electricity Price Index 2018. https://www1.electricityinfo.co.nz/price_indexes (accessed March 1, 2018).

[59] Lefort A, Bourdais R, Ansanay-Alex G, Guéguen H. Hierarchical control method applied to energy management of a residential house. Energy Build 2013;64:53–61. doi:10.1016/j.enbuild.2013.04.010.